Korean J. Chem. Eng., 32(8), 1678-1687 (2015)
DOI: 10.1007/s11814-014-0378-7

pISSN: 0256-1115
eISSN: 1975-7220

Measurement of CO_2 solubility in cyanide anion based ionic liquids; $[c_4mim][SCN]$, $[c_4mim][N(CN)_2]$, $[c_4mim][C(CN)_3]$

Ji Eun Kim*, Jeong Won Kang, and Jong Sung Lim*,†**

*Department of Chemical and Biomolecular Engineering, Sogang University, 1, Sinsu-dong, Mapo-gu, Seoul 121-742, Korea
**Department of Chemical and Biological Engineering, Korea University, 5-1, Anam-dong, Sungbuk-gu, Seoul 136-701, Korea
(*Received 14 October 2014 • accepted 17 December 2014*)

Abstract−To investigate the effect of cyanide ions on the solubility of CO_2 in ionic liquid, we measured the solubility of CO_2 in three ionic liquids which contain three different numbers of cyanide anions, 1-butyl-3-methylimidazolium thiocyanate ($[c_4mim][SCN]$), 1-butyl-3-methylimidazolium dicyanamide ($[c_4mim][N(CN)_2]$) and 1-butyl-3-methylimidazolium tricyanomethanide ($[c_4mim][C(CN)_3]$). The solubility of CO_2 in ionic liquids was determined by measuring bubble-point pressure in high-pressure variable-volume view cell at temperatures from 303.15 to 373.15 K in 10 K intervals. The measured data were correlated with the Peng-Robinson equation of state (PR-EoS) using the van der Waals one fluid mixing rules. The critical properties and acentric factor of ionic liquids were estimated by using the modified Lydersen-Joback-Reid method. As a result, the calculated data were relatively well agreed with the experimental results and, as is commonly known, the solubility of CO_2 was observed to increase with increasing pressure and with decreasing temperature. The results also show that the highest solubility was obtained by $[c_4mim][C(CN)_3]$ among those three experimented ionic liquids while $[c_4mim][SCN]$ had the lowest. This implies that the CO_2 solubility is affected by the number of cyanide anions contained in ionic liquid. From this result, it is concluded that the cyanide anion enhances the CO_2 solubility in ionic liquid and that the ionic liquid which contains more cyanide anions has higher CO_2 solubility.

Keywords: Ionic Liquids, Solubility, Carbon Dioxide, Cyanide Anion, Carbon Capture

INTRODUCTION

Ionic Liquids (ILs), which generally consist of organic cation and anion, are fluid at room temperature [1]. Melting points of ILs are affected by the electrostatic potential, which is related to the lattice energy. Unbalanced structure of ion pairs, in which there is a different size and shape of cation and anion, decreases lattice energy and, thereby ILs have melting points near room temperature [2,3]. ILs have attracted increasing attention since they have unique and peculiar physicochemical properties such as no measurable vapor pressure, high thermal stability, and high electric conductivity. [1,4,5]. In addition, ionic liquid is called "designer solvent," which means ionic liquid can synthesize cation and anion freely in order to adjust specific function of ionic liquid [5].

There have been many studies showing that ILs are potential to be useful in major fields of application. Kohoutova et al. [6] reported the stability and selectivity of polymer-ionic liquid membrane. Benzagouta et al. [7] suggested ionic liquid has a possibility for potential use in surfactant. Recent studies have shown that ionic liquid has the catalytic ability to replace existing catalysis and there, also, are a wide potential of applications in electrolyte, enzyme, and so on [8-10]. Among the diverse applications, a number of studies related to CO_2 capture system using ILs are currently underway. In particular, many technologies for capturing CO_2 have already been developed in recent decades, and capturing CO_2 technology using aqueous amine is generally used in natural gas sweetening process in power plant. Chemical reaction between amine and CO_2 occurs and aqueous amine selectively captures CO_2 from other gases [11,12]. However, this process has several drawbacks such as energy efficiency for regeneration, corrosiveness and pyrolysis of solvent at high temperature [13]. To overcome these problems, ILs have been suggested as alternative materials to capture CO_2 because ILs have effective solubility of many compounds as well as properties mentioned above. Especially, ILs separate CO_2 selectively from other gases including N_2, O_2, and so on due to high solubility of CO_2 in ILs [1,4,5]. Many researchers have suggested solubility of CO_2 in various ionic liquids containing imidazolium, pyridinium, pyrrolidinium based cations and different anions by changing combination of cation and anion [14,15], and it is required to carry out investigation about solubility of CO_2 in various kinds of ionic liquids continually. We have studied solubility of CO_2 in ionic liquids with cyanide anions and reported 1-ethyl-3-methylimidzolium-based ionic liquids containing cyanide anions in our previous work [16].

The aim of present study is to measure solubility of CO_2 in three ionic liquids containing different numbers of cyanide anion and to understand the effect of cyanide anion in ionic liquids on CO_2 solubility. The solubilities of CO_2 in three different ionic liquids, 1-butyl-3-methylimidazolium thiocyanate ($[c_4mim][SCN]$), 1-butyl-

†To whom correspondence should be addressed.
E-mail: limjs@sogang.ac.kr
‡This article is dedicated to Prof. Hwayong Kim on the occasion of his retirement from Seoul National University.

3-methylimidazolium dicyanamide ([$c_4$mim][$N(CN)_2$]) and 1-butyl-3-methylimidazolium tricyanomethanide ([$c_4$mim][$C(CN)_3$]), were determined by measuring the bubble-point pressure (or cloud-point pressure) in high-pressure variable-volume view cell at a temperature range from 303.15 to 373.15 K in 10 K intervals. Then, measured data was correlated with the Peng-Robinson equation of state (PR-EoS) using the conventional van der Waals one fluid mixing rules. This study also discusses the effect of alkyl chain group length in cation on solubility of CO_2 by comparing solubility of CO_2 in [$c_4$mim] cation-based ionic liquids with that in [$c_2$mim] cation-based ionic liquid from our previous work [16].

EXPERIMENTAL

1. Materials

The ionic liquids [$c_4$mim][$C(CN)_3$], [$c_4$mim][$N(CN)_2$] and [$c_4$mim][SCN] were purchased from Future Chem (Korea). The chemical structures of [$c_4$mim][SCN], [$c_4$mim][$N(CN)_2$] and [$c_4$mim][$C(CN)_3$] are shown in Fig. 1. To reduce the water content and to eliminate other gases, the ionic liquid sample was placed into high-pressure variable-volume view cells for solubility measurement and evacuated by vacuum pump for several days. Coulometric Karl Fischer titration (Metrohm model 684) was performed on a sample of the evacuated ionic liquids. The high-purity (99.999 mass %) carbon dioxide was purchased from Dong-A Gas Co. (Korea). The ionic liquids and CO_2 gas were used without further purification. The purity data for ionic liquids and CO_2 are listed in Table 1.

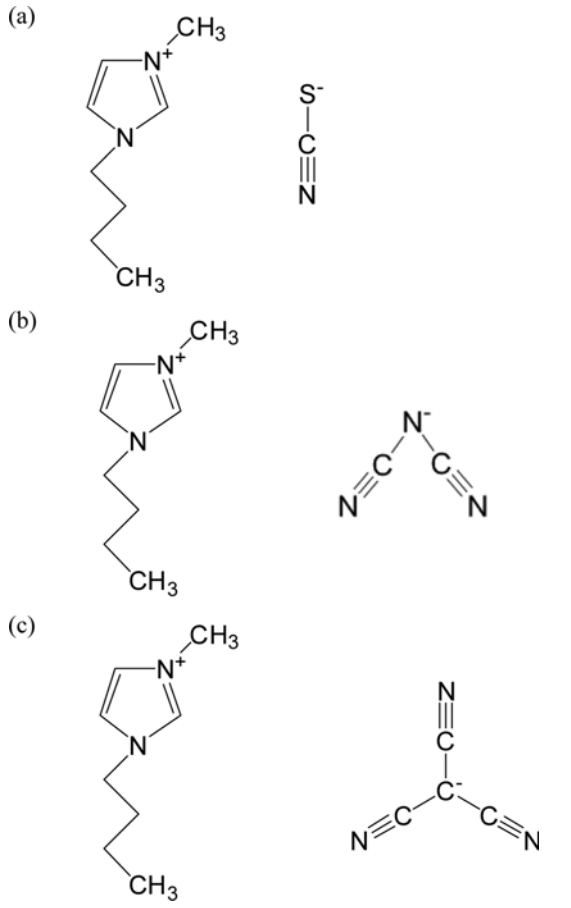

Fig. 1. Chemical structure of ionic liquids: (a) [$c_4$mim][SCN], (b) [$c_4$mim][$N(CN)_2$], and (c) [$c_4$mim][$C(CN)_3$].

2. Experimental Apparatus

The schematic diagram of the experiment apparatus is shown in Fig. 2. The solubility measurement apparatus used in this study is identical to the one used in our previous works [16-19]. The solubility of CO_2 in ionic liquids was measured using a high-pressure variable-volume view cell. The heart of the system is the high-pressure variable-volume view cell. The focal aspect of the variable-volume cell apparatus is its ability to keep the contents of the cell constant throughout the duration of the experiment. The cell has a dimension of 16 mm i.d.×70 mm o.d. and an internal working volume of about 31 cm^3. A piston is placed inside the cell to alter the

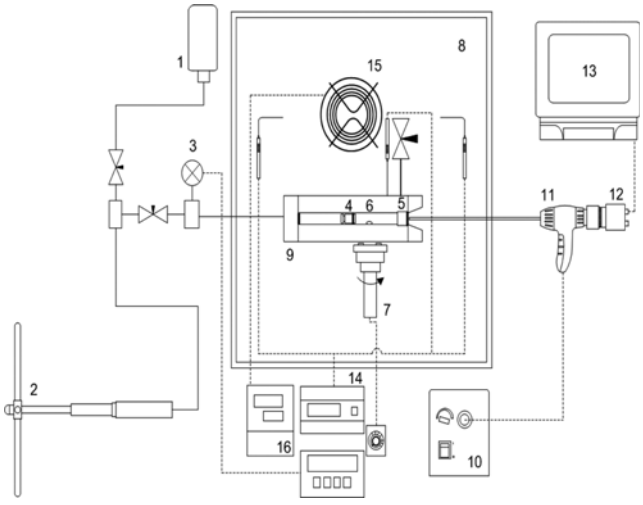

Fig. 2. A schematic diagram of the experimental apparatus.

1. Water for pressing	9. Variable-volume view cell
2. Pressure generator	10. Light source
3. Pressure gauge	11. Borescope
4. Piston	12. CCD camera
5. Sapphire window	13. Monitor
6. Magnetic bar	14. Temperature gauge
7. Stirrer	15. Heater
8. Air bath	16. Heating controller

Table 1. Purity data of ionic liquids

Ionic liquids	Source	Assay (mass%)	Halides content (%)	Initial water content (PPM)	Water removal method	Final water content (PPM)	Water analysis method
[$c_4$mim][SCN]	Future-Chem	98	1.06	1220	Vacuum evaporation	22	Karl Fischer titration
[$c_4$mim][$N(CN)_2$]	Future-Chem	98	0.79	1870	Vacuum evaporation	25	Karl Fischer titration
[$c_4$mim][$C(CN)_3$]	Future-Chem	98	0.38	130	Vacuum evaporation	17	Karl Fischer titration

cell volume. A pressure generator (High Pressure Equipment Co. model 50-6-15) is used to pressurize the water and then displace the piston. Any change in the cell volume causes a change in the system pressure. A sapphire window is inserted into the view cell to facilitate visual observation of the cell interior. The system pressure is measured using a high-precision pressure gauge (Dresser Heise model CC-12-G-A-02B, ±0.05 MPa accuracy, ±0.01 MPa resolution) placed between the pressure generator and the view cell. The system temperature is measured to be within ±0.1 K of the set temperature when an RTD temperature probe is inserted into the cell. A temperature-controlled forced-convection air bath is used to keep the system temperature constant. Visual observation of the cell interior through the sapphire window is achieved via borescope (Olympus model R080-044-000-50) and CCD camera connected to a monitor. A magnetic stirring system is installed under the cell body to mix the contents of the cell. A stirring bar in the cell is activated by a samarium-cobalt magnet located below the cell, and the magnet is powered by an electric motor.

3. Experimental Procedure

Ionic liquid sample was loaded into the high-pressure variable-volume view cell. The sample was approximately 8-9 g, providing sufficient space to agitate the stirring bar in the variable-view cell. The piston, stirring bar and sapphire window were inserted into the variable-view cell. The piston created the space inside the cell using a pressure generator that was used to pressurize the water. We observed the cell interior though the sapphire window. To remove any air trapped in the cell as well as any other dissolved gas and water in the ionic liquid, the cell was evacuated by vacuum pump at room temperature for several days before the experiment. Once the air space of the system was fully evacuated, a designated amount of CO_2 was loaded into cell. The exact amount of CO_2 gas introduced into the cell was determined by weighing the CO_2 sample cylinder before and after loading using a balance (Precias model 1,212 M) with an accuracy of 1 mg. To prevent any loss of CO_2 gas in the feed line during loading, the CO_2 gas in the feed line was stored in the CO_2 sample cylinder by dipping the cylinder into a Dewar flask filled with liquid nitrogen. The margin of error in measuring the ionic liquids and CO_2 was ±0.2 mg and ±2 mg, respectively. The uncertainty analysis for the composition measurement of each component was analyzed to be within ±0.007 mole fractions and was performed in accordance with the International Organization of Standardization (ISO) guidelines [20]. The mole fraction of the CO_2 in the ionic liquid was calculated based on the known amount of CO_2. To dissolve CO_2 in ionic liquid, the ionic liquid-CO_2 mixture was agitated with a stirring bar. As the pressure increased, the CO_2 and ionic liquid mixture in the cell reached a single phase, after which the pressure was slowly reduced until the first CO_2 bubble was observed in the solution or the cell interior became clouded. At this moment, we measured the pressure of the cell and noted it as the bubble-point pressure or cloud-point pressure at a fixed CO_2 mole fraction and temperature. The pressure reduction rates for the determinations of the bubble-point pressure ranged from approximately 0.05 $MPas^{-1}$ for the highest bubble-point pressure case to 0.001 $MPas^{-1}$ for the lowest bubble-point pressure case. The reduction rate was very slow such that the effects of the rate on the results of the bubble-point pressure were not observed. After one set of experiments from 303.15 to 373.15 K was performed on a fixed CO_2 mole fraction, more CO_2 was charged into the cell and the CO_2 mole fraction for the new experiment system was recalculated. The successive experiments with increasing CO_2 mole fractions were performed as outlined in this procedure. Every measurement was repeated more than three times at each temperature to obtain accurate data. The uncertainty of the temperature measurement was ±0.1 K and of the bubble-point pressure measurement was 0.06 MPa.

THERMODYNAMIC MODELING

The experimental (CO_2+ionic liquid) data correlated with the Peng-Robinson equation of state (PR-EoS) [21]. The mixture parameters in the ionic liquid phase were calculated with the conventional van der Waals one fluid mixing rules. The detailed explanation of the PR-EoS and the conventional van der Waals one fluid mixing rules was reported in our previous works [18,19]. The normal boiling temperature (T_b), critical temperature (T_c), critical pressure (P_c) and acentric factor (ω) of the ionic liquid and the CO_2 were used to calculate the parameters for the PR-EoS. These properties of the CO_2 were available from the literature [22]. However, the properties of the ionic liquids are unknown. Therefore, the critical properties of the ionic liquids had to be estimated. In this work, one of the group contribution methods, the modified Lydersen-Joback-Reid method, is used to estimate critical properties and obtain definite results for molecules with high molecular weights. The groups considered for the modified Lydersen-Joback-Reid method are presented in the referenced works [23]. The acentric factor was calculated based on critical properties and normal boiling temperature (T_b for P_b=0.1 MPa). All the critical properties, the normal boiling temperature and the acentric factors of the ionic liquids and the CO_2 are listed in Table 2.

RESULTS AND DISCUSSION

In this work, the solubility of CO_2 in three ionic liquids was measured at eight temperatures range from 303.15 to 373.15 K in 10 K intervals. Each ionic liquid used in this study combined 1-butyl-3-methylimidazolium cation ([$c_4$mim]) with three anions containing different numbers of cyanide ([SCN], [$N(CN)_2$] or [$C(CN)_3$]). The experimental results for the CO_2+[$c_4$mim][SCN], [$c_4$mim][$N(CN)_2$], and [$c_4$mim][$C(CN)_3$] are shown in Tables 3-5, respectively. These tables present measured bubble-point (or cloud-point) pressure for each dissolved mole fraction of CO_2 in the ionic liquid. When the

Table 2. Thermodynamic properties of CO_2 from reference literature [22] and ionic liquids calculated from modified Lydersen-Joback-Reid method [23]

	M (g/mol)	T_b (K)	T_c (K)	P_c (MPa)	ω
CO_2	44	-	304.21	7.3847	0.2239
[$c_4$mim][SCN]	197.3	763.08	1047.36	1.9384	0.4781
[$c_4$mim][$N(CN)_2$]	205.26	782.96	1035.84	2.4400	0.8419
[$c_4$mim][$C(CN)_3$]	229.28	915.06	1184.98	2.1136	0.9266

Table 3. Solubility data for the [$c_4$mim][SCN]+CO_2 system[a]

x (CO_2)	T (K)	P (MPa)	Phase state of CO_2	x (CO_2)	T (K)	P (MPa)	Phase state of CO_2
0.159	303.15	0.70	b[b]	0.422	303.15	8.61	c[c]
	313.15	0.97	b		313.15	12.25	c
	323.15	1.26	b		323.15	15.93	c
	333.15	1.64	b		333.15	19.28	c
	343.15	2.12	b		343.15	22.36	c
	353.15	2.41	b		353.15	25.39	c
	363.15	2.77	b		363.15	28.13	c
	373.15	3.19	b		373.15	30.56	c
0.198	303.15	1.39	b	0.454	303.15	15.97	c
	313.15	1.88	b		313.15	20.25	c
	323.15	2.33	b		323.15	23.85	c
	333.15	2.80	b		333.15	27.46	c
	343.15	3.46	b		343.15	30.77	c
	353.15	3.96	b		353.15	33.65	c
	363.15	4.75	b		363.15	36.37	c
	373.15	5.46	b		373.15	38.86	c
0.248	303.15	1.88	b	0.465	303.15	23.43	c
	313.15	2.71	b		313.15	27.71	c
	323.15	3.59	b		323.15	31.52	c
	333.15	4.33	b		333.15	35.13	c
	343.15	5.04	b		343.15	38.40	c
	353.15	5.93	b		353.15	41.31	c
	363.15	6.78	b		363.15	43.95	c
	373.15	7.58	b		373.15	46.49	c
0.294	303.15	3.39	b	0.485	303.15	41.69	c
	313.15	4.22	b		313.15	45.66	c
	323.15	5.22	b		323.15	48.65	c
	333.15	6.24	b		333.15	51.83	c
	343.15	7.34	b		343.15	54.78	c
	353.15	8.38	b		353.15	57.33	c
	363.15	9.44	b		363.15	59.74	c
	373.15	10.80	b		373.15	61.93	c
0.345	303.15	3.75	b	0.498	303.15	58.72	c
	313.15	4.97	b		313.15	61.81	c
	323.15	5.97	b		323.15	64.23	c
	333.15	8.30	b		333.15	66.92	c
	343.15	10.18	b		343.15	69.44	c
	353.15	12.37	b		353.15	71.73	c
	363.15	14.46	b		363.15	73.72	c
	373.15	16.29	b		373.15	75.45	c
0.381	303.15	5.04	b	0.514	303.15	81.57	c
	313.15	6.42	b		313.15	84.72	c
	323.15	8.56	b		323.15	87.42	c
	333.15	10.79	b		333.15	90.09	c
	343.15	13.64	b		343.15	91.93	c
	353.15	15.87	b		353.15	93.09	c
	363.15	18.41	b		363.15	94.26	c
	373.15	20.72	b		373.15	95.46	c

[a]Standard uncertainties u are u(T)=±0.1 K, u(P)=±0.06 MPa and u(x)=±0.007 mole fractions
[b]Bubble point [c]Cloud point

Table 4. Solubility data for the $[c_4mim][N(CN)_2]+CO_2$ system[a]

x (CO_2)	T (K)	P (MPa)	Phase state of CO_2	x (CO_2)	T (K)	P (MPa)	Phase state of CO_2
0.174	303.15	0.82	b[b]	0.550	303.15	8.84	c[c]
	313.15	0.98	b		313.15	13.67	c
	323.15	1.21	b		323.15	18.46	c
	333.15	1.42	b		333.15	23.27	c
	343.15	1.79	b		343.15	27.69	c
	353.15	2.16	b		353.15	31.61	c
	363.15	2.50	b		363.15	35.06	c
	373.15	2.96	b		373.15	38.76	c
0.239	303.15	1.41	b	0.579	303.15	20.46	c
	313.15	1.74	b		313.15	25.92	c
	323.15	2.17	b		323.15	31.16	c
	333.15	2.69	b		333.15	35.18	c
	343.15	3.18	b		343.15	39.32	c
	353.15	3.62	b		353.15	42.99	c
	363.15	4.27	b		363.15	45.36	c
	373.15	4.83	b		373.15	47.45	c
0.301	303.15	2.15	b	0.594	303.15	23.33	c
	313.15	2.65	b		313.15	28.90	c
	323.15	3.17	b		323.15	34.45	c
	333.15	3.82	b		333.15	39.53	c
	343.15	4.38	b		343.15	43.91	c
	353.15	5.11	b		353.15	48.03	c
	363.15	5.82	b		363.15	51.47	c
	373.15	6.37	b		373.15	54.76	c
0.354	303.15	2.71	b	0.616	303.15	32.81	c
	313.15	3.30	b		313.15	38.88	c
	323.15	3.96	b		323.15	45.11	c
	333.15	4.84	b		333.15	50.08	c
	343.15	5.78	b		343.15	55.28	c
	353.15	6.56	b		353.15	60.00	c
	363.15	7.65	b		363.15	63.86	c
	373.15	8.64	b		373.15	67.48	c
0.417	303.15	3.57	b	0.634	303.15	55.31	c
	313.15	4.48	b		313.15	58.71	c
	323.15	5.53	b		323.15	64.05	c
	333.15	6.73	b		333.15	68.23	c
	343.15	7.92	b		343.15	72.81	c
	353.15	9.24	b		353.15	77.25	c
	363.15	10.87	b		363.15	81.11	c
	373.15	12.61	b		373.15	84.71	c

[a]Standard uncertainties u are u(T)=±0.1 K, u(P)=±0.06 MPa and u(x)=±0.007 mole fractions
[b]Bubble point
[c]Cloud point

mole fraction of CO_2 is less than 0.422 in the $[c_4mim][SCN]$, 0.550 in the $[c_4mim][N(CN)_2]$ and 0.668 in the $[c_4mim][C(CN)_3]$, the phase separation behavior is observed as bubble-point even at temperature above the critical point of CO_2; on the other hand, when the mole fraction of CO_2 is more than 0.422 mole fractions of CO_2 in the $[c_4mim][SCN]$, 0.550 in the $[c_4mim][N(CN)_2]$ and 0.668 in the $[c_4mim][C(CN)_3]$, the phase separation behaviour is observed as cloud-point. These behaviors can be explained by high density of CO_2. As the mole fraction of CO_2 becomes increased, CO_2 behaves as liquid, and thus, separation phenomenon into CO_2 and ionic liquid occurs close to vapor-liquid equilibrium rather than to liquid-liquid equilibrium [24,25]. Fig. 3 shows the relation between

Table 4. Continued

x (CO_2)	T (K)	P (MPa)	Phase state of CO_2	x (CO_2)	T (K)	P (MPa)	Phase state of CO_2
0.475	303.15	4.42	b	0.641	303.15	59.65	c
	313.15	5.68	b		313.15	66.53	c
	323.15	7.59	b		323.15	71.04	c
	333.15	10.02	b		333.15	75.13	c
	343.15	12.56	b		343.15	79.35	c
	353.15	15.77	b		353.15	83.44	c
	363.15	19.00	b		363.15	86.46	c
	373.15	21.88	b		373.15	89.47	c
0.514	303.15	5.33	b				
	313.15	7.00	b				
	323.15	10.07	b				
	333.15	14.01	b				
	343.15	17.98	b				
	353.15	21.31	b				
	363.15	24.85	b				
	373.15	28.11	b				

[a]Standard uncertainties u are u(T)=±0.1 K, u(P)=±0.06 MPa and u(x)=±0.007 mole fractions
[b]Bubble point
[c]Cloud point

Table 5. Solubility data for the [$c_4$mim][$C(CN)_3$]+CO_2 system[a]

x (CO_2)	T (K)	P (MPa)	CO_2 observed	x (CO_2)	T (K)	P (MPa)	CO_2 observed
0.157	303.15	0.40	b[b]	0.633	303.15	6.86	b
	313.15	0.50	b		313.15	10.46	b
	323.15	0.64	b		323.15	14.85	b
	333.15	0.81	b		333.15	19.42	b
	343.15	1.02	b		343.15	23.52	b
	353.15	1.23	b		353.15	27.53	b
	363.15	1.40	b		363.15	31.14	b
	373.15	1.70	b		373.15	34.70	b
0.261	303.15	1.06	b	0.668	303.15	17.01	c[c]
	313.15	1.37	b		313.15	22.27	c
	323.15	1.59	b		323.15	27.56	c
	333.15	1.86	b		333.15	32.35	c
	343.15	2.25	b		343.15	37.15	c
	353.15	2.73	b		353.15	41.16	c
	363.15	3.19	b		363.15	45.36	c
	373.15	3.62	b		373.15	49.05	c
0.325	303.15	1.64	b	0.687	303.15	23.15	c
	313.15	2.02	b		313.15	29.11	c
	323.15	2.48	b		323.15	34.27	c
	333.15	2.97	b		333.15	39.56	c
	343.15	3.54	b		343.15	44.20	c
	353.15	4.20	b		353.15	48.76	c
	363.15	4.88	b		363.15	52.87	c
	373.15	5.40	b		373.15	56.87	c

[a]Standard uncertainties u are u(T)=±0.1 K, u(P)=±0.06 MPa and u(x)=±0.007 mole fractions
[b]Bubble point
[c]Cloud point

Table 5. Continued

x (CO_2)	T (K)	P (MPa)	CO_2 observed	x (CO_2)	T (K)	P (MPa)	CO_2 observed
0.390	303.15	2.41	b	0.706	303.15	34.79	c
	313.15	2.92	b		313.15	40.54	c
	323.15	3.62	b		323.15	46.21	c
	333.15	4.21	b		333.15	51.89	c
	343.15	4.97	b		343.15	56.10	c
	353.15	5.77	b		353.15	60.76	c
	363.15	6.61	b		363.15	65.02	c
	373.15	7.73	b		373.15	69.23	c
0.453	303.15	3.07	b	0.730	303.15	52.00	c
	313.15	3.81	b		313.15	58.15	c
	323.15	4.57	b		323.15	64.27	c
	333.15	5.44	b		333.15	69.54	c
	343.15	6.39	b		343.15	74.44	c
	353.15	7.60	b		353.15	79.19	c
	363.15	8.75	b		363.15	83.44	c
	373.15	9.91	b		373.15	87.71	c
0.502	303.15	3.79	b	0.741	303.15	61.90	c
	313.15	4.63	b		313.15	67.89	c
	323.15	5.61	b		323.15	73.67	c
	333.15	6.81	b		333.15	79.29	c
	343.15	7.92	b		343.15	84.19	c
	353.15	9.32	b		353.15	89.15	c
	363.15	11.05	b		363.15	93.33	c
	373.15	13.19	b		373.15	97.30	c
0.569	303.15	4.70	b				
	313.15	5.74	b				
	323.15	7.57	b				
	333.15	9.81	b				
	343.15	12.53	b				
	353.15	15.19	b				
	363.15	17.76	b				
	373.15	20.62	b				

[a]Standard uncertainties u are u(T)=±0.1 K, u(P)=±0.06 MPa and u(x)=±0.007 mole fractions
[b]Bubble point
[c]Cloud point

Table 6. Binary interaction parameters (k_{12}, l_{12}) for ionic liquids system[a]

Temperature	[$c_4$mim][SCN]		[$c_4$mim][$N(CN)_2$]		[$c_4$mim][$C(CN)_3$]	
	k_{12}	l_{12}	k_{12}	l_{12}	k_{12}	l_{12}
303.15 K	0.29501	0.07529	0.10502	0.04086	0.06795	0.03867
313.15 K	0.28405	0.06400	0.11025	0.04241	0.06986	0.03925
323.15 K	0.28020	0.05725	0.11379	0.04226	0.07172	0.03916
333.15 K	0.27376	0.04939	0.11636	0.04144	0.07377	0.03930
343.15 K	0.26561	0.04108	0.11906	0.04070	0.07481	0.03873
353.15 K	0.27371	0.04076	0.12339	0.04134	0.07595	0.03825
363.15 K	0.27620	0.03785	0.12738	0.04151	0.07795	0.03884
373.15 K	0.27855	0.03495	0.12944	0.04121	0.07911	0.03834

[a]Standard uncertainties u are u(T)=±0.1 K andu(P)=±0.06 MPa

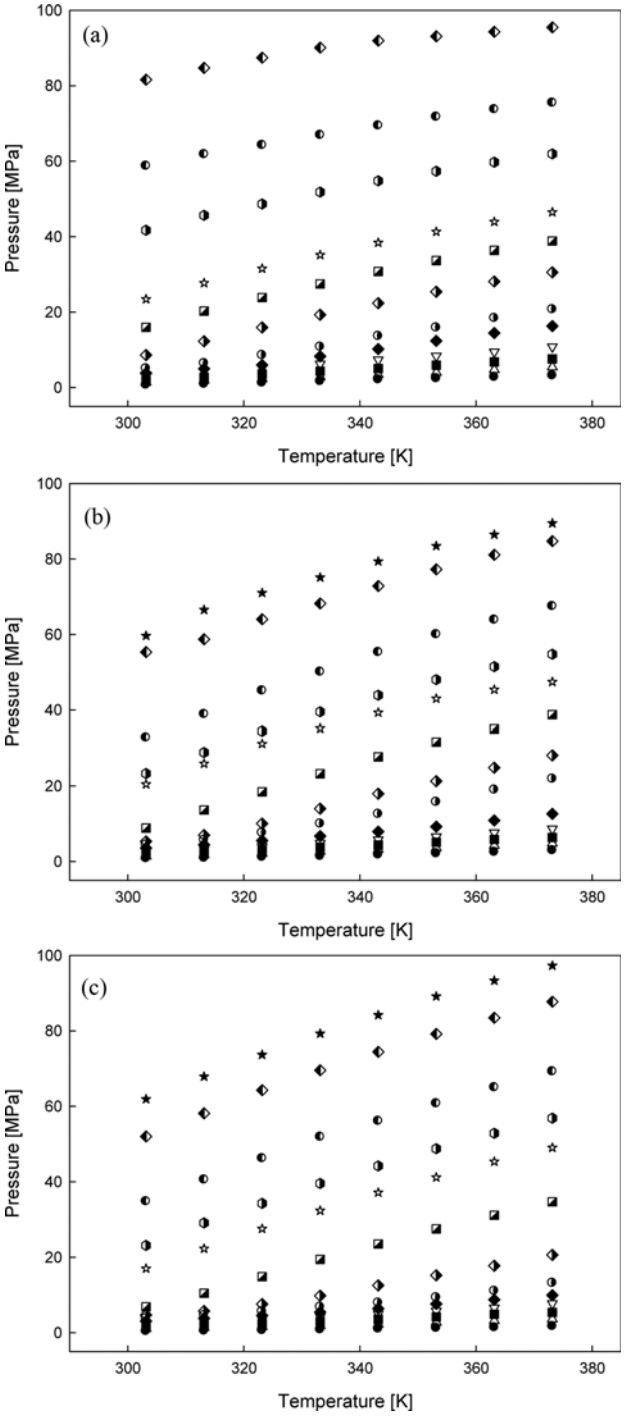

Fig. 3. P-T diagram of CO_2 solubilities of the (ionic liquid+CO_2) system: (a) [$c_4$mim][SCN]+CO_2. The symbols are CO_2 mole fractions as defined: ●, 0.1591; △, 0.1981; ■, 0.2477; ▽, 0.2943; ◆, 0.3446; ◑, 0.3808; ◗, 0.4222; ◪, 0.4537; ☆, 0.4645; ◗, 0.4848; ◐, 0.4984; ◖, 0.5138. (b) [$c_4$mim] [$N(CN)_2$]+CO_2. The symbols are CO_2 mole fractions as de- fined: ●, 0.1738; △, 0.2385; ■, 0.3007; ▽, 0.3535; ◆, 0.4170; ◑, 0.4752; ◗, 0.5137; ◪, 0.5498; ☆, 0.5788; ◗, 0.5941; ◐, 0.6160; ◖, 0.6343, ★, 0.6408. (c) [$c_6$mim][$C(CN)_3$] +CO_2. The symbols are CO_2 mole fractions as defined: ●, 0.1574; △, 0.2612; ■, 0.3245; ▽, 0.3904; ◆, 0.4528; ◑, 0.5019; ◗, 0.5692; ◪, 0.6325; ☆, 0.6683; ◗, 0.6870; ◐, 0.7061; ◖, 0.7299, ★, 0.7411.

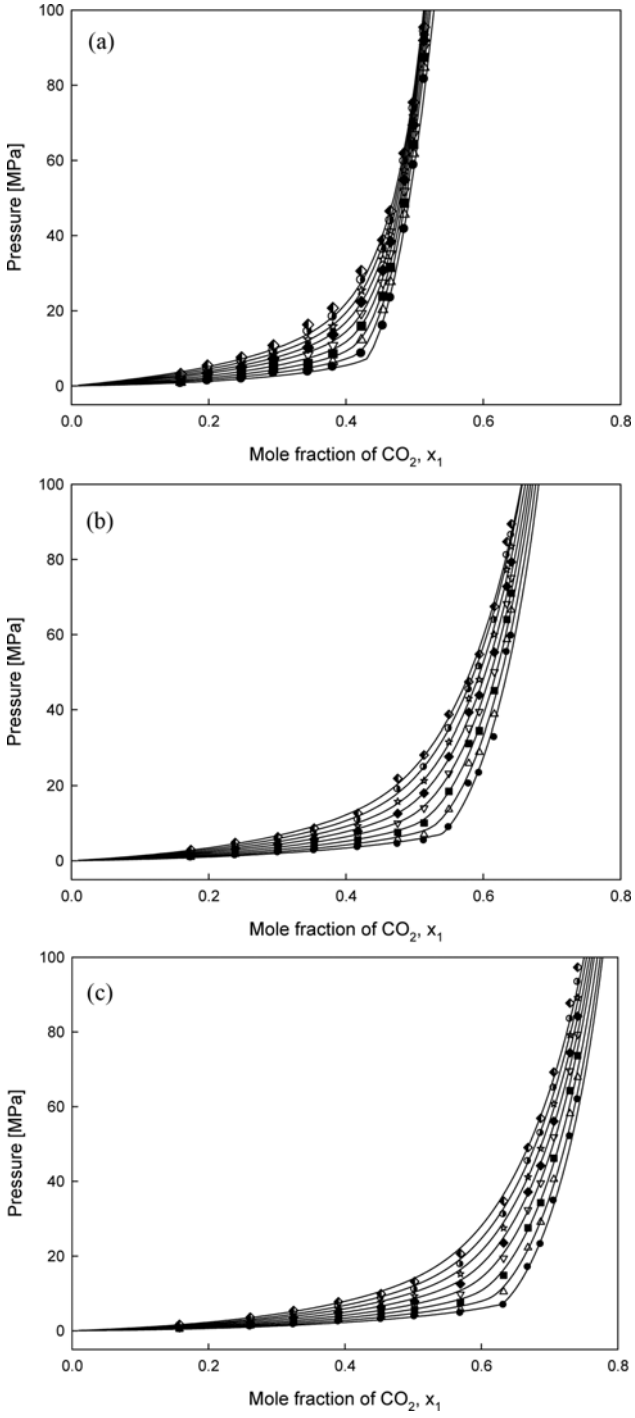

Fig. 4. P-x_1 diagram of CO_2 solubilities of the (ionic liquid+CO_2) system: (a) [$c_4$mim][SCN]+CO_2; (b) [$c_4$mim][$N(CN)_2$]+CO_2; (c)[$c_4$mim][$C(CN)_3$]+CO_2. The symbols represent the temperatures: ●, 303.15 K; △, 313.15 K; ■, 323.15 K; ▽, 333.15 K; ◆, 343.15 K; ☆, 353.15 K; ◑, 363.15 K; and ◖, 373.15 K; (-), as calculated by the PR-EoS model.

solubility of CO_2 and the temperature. It illustrates bubble-point (or cloud-point) pressure linearly increased with increasing temperature at fixed mole fractions of CO_2, as is commonly known.

The experimental data were correlated with the PR-EoS incorporated with the van der Waals one fluid mixing rules. Calculated

Table 7. Average absolute deviations of pressure (AAD-*P* %) between experiment data and calculated values for the (ionic liquid+CO_2) system[a]

Temperature	AAD-P^b %		
	$[c_4mim][SCN]$	$[c_4mim][N(CN)_2]$	$[c_4mim][C(CN)_3]$
303.15 K	9.08	7.40	6.14
313.15 K	9.19	6.47	6.79
323.15 K	9.15	5.01	5.65
333.15 K	8.80	4.04	4.23
343.15 K	7.79	3.03	4.54
353.15 K	8.00	3.47	4.68
363.15 K	8.03	4.20	4.56
373.15 K	7.52	4.35	4.34
Average	8.45	4.75	5.12

[a]Standard uncertainties u are u(T)=±0.1 K and u(P)=±0.06 MPa
[b]Average absolute deviation in percentage:
$AAD(\%)=(1/N)\Sigma_{i=1}^{N}|(P_i^{calc}-P_i^{exp})/P_i^{exp}|\times 100$ (N=number of data point)

binary interaction parameters for each system at temperatures from 303.15 to 373.15 K in 10 K intervals are given in Table 6. Fig. 4 indicates the equilibrium pressure we obtain in experiment and the fitted value of experimental data versus the mole fraction of CO_2. Although the calculated results deviate from the experimental data as mole fraction of CO_2 increases, the calculated results were found in close accordance with the experimental data. The average absolute deviations of pressure (AAD-*P* %) between the experiment data and the calculated results for each system are reported in Table 7. The overall average values of AAD-*P* (%) through the temperatures range from 303.15 to 373.15 K were 8.45% for $[c_4mim][SCN]$, 4.75% for $[c_4mim][N(CN)_2]$ and 5.12% for $[c_4mim][C(CN)_3]$.

As can be seen in Fig. 4, the equilibrium pressure shows a steadily increasing curve under 0.43 mole fraction of CO_2 in $[c_4mim][SCN]$, 0.54 in $[c_4mim][N(CN)_2]$ and 0.63 in $[c_4mim][C(CN)_3]$ at constant temperature. But, at higher mole fraction of CO_2, equilibrium curve marks a steep rise. It seems possible to fill space within ionic liquid with CO_2 at low mole fraction of CO_2, but there is little space which filled with CO_2 at high mole fraction of CO_2 [26]. When equilibrium pressure is associated with separation phase behavior observed, the bubble-point is observed with increasing equilibrium pressure gradually, while the cloud-point is observed with increasing equilibrium pressure sharply. Fig. 5 illustrates a comparison of CO_2 solubility data in this work with those in the literatures. Revelli, et al. [27] examined CO_2 solubility in [c4mim][SCN] and Carvalho, et al. [28] reported CO_2 solubility in $[c4mim][N(CN)_2]$. It is shown that good agreement exists between the experimental data and literature data.

Fig. 6 shows a comparison of CO_2 solubility in ionic liquids containing the different cyanide anion at 333.15 K. $[c_4mim][C(CN)_3]$ has the highest CO_2 solubility, followed by $[c_4mim][N(CN)_2]$ and then $[c_4mim][SCN]$ at fixed pressure.It meant that cyanide anion in the ionic liquids play an important role in the CO_2 solubility. It is believed that there exists weak electrostatic interaction between cation and anion, and when CO_2 is soluble in ionic liquids, the Lewis

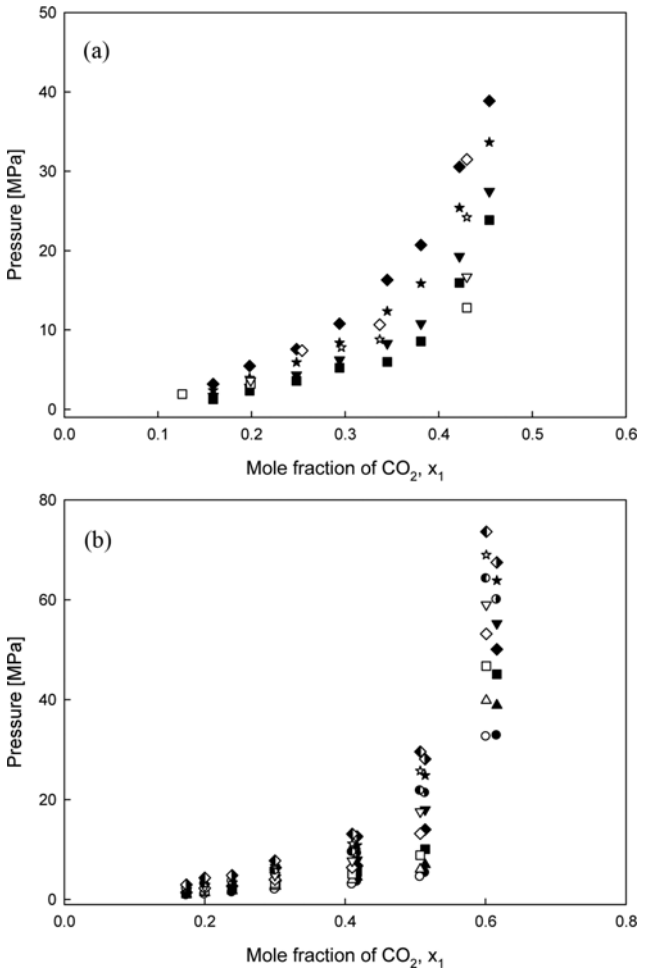

Fig. 5. Comparison of our CO_2 solubility data with literature values: (a) $[c_4mim][SCN]+CO_2$. The symbols represent the temperatures: ■, 323.15 K; ▼, 333.15 K; ★, 353.15 K; ◆, 373.15 K; □, 323.15 K [27]; ▽, 333.15 K [27]; ☆, 353.15 K [27]; ◇, 373.15 K [27]; (b) $[c_4mim][N(CN)_2]+CO_2$. The symbols represent the temperatures: ●, 303.15 K; ▲, 313.15 K; ■, 323.15 K; ◆, 333.15 K; ▼, 343.15 K; ◑, 353.15 K; ★, 363.15 K; ◭, 373.15 K; ○, 303.15 K [28]; △, 313.15 K [28]; □, 323.15 K [28]; ◇, 333.15 K [28]; ▽, 343.15 K [28]; ◐, 353.15 K [28]; ☆, 363.15 K [28]; ◭, 373.15 K [28].

acid-base interaction between CO_2 molecules and ionic liquids molecules is formed by acting the CO_2 as Lewis acid and cyanide anion cyanide anion in the ionic liquid as a Lewis base. The more the cyanide anion in ionic liquids, the larger interaction between CO_2 molecules and ionic liquid molecules became, and thus, ionic liquids have higher solubility of CO_2 [26,29]. Fig. 6 also, illustrates effects of alkyl group chain in cation on solubility of CO_2. It compares the current study with results about 1-ethyl-3-methylimidazolium ($[c_2mim]$) based ionic liquids from previous work [16], and presents that solubility of CO_2 increases as alkyl chain group length increases. The dissolved CO_2 mole fractions in $[c_2mim][C(CN)_3]$, $[c_2mim][N(CN)_2]$ and $[c_2mim][SCN]$ are about 0.70, 0.60, and 0.45. On the other hand, the CO_2 mole fractions in $[c_4mim][C(CN)_3]$, $[c_4mim][N(CN)_2]$ and $[c_4mim][SCN]$ are about 0.75, 0.65, and 0.50 at 80 MPa, respectively. The densities of ILs decrease as alkyl chain

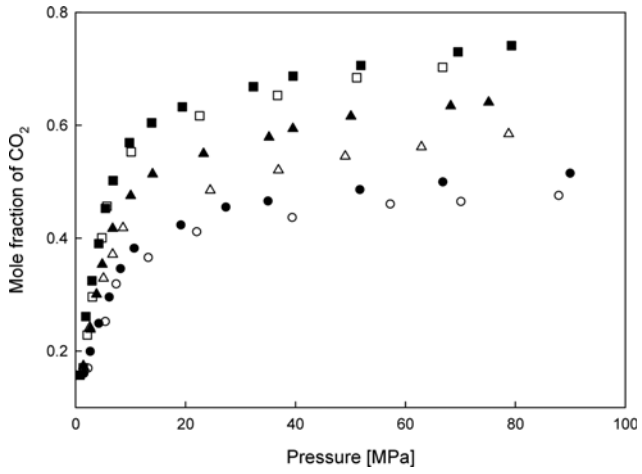

Fig. 6. Comparison of CO_2 solubilities between the various cyanide anion based ionic liquids at 333.15 K. The symbols are ionic liquids: ●, [$c_4$mim][SCN]; ▲, [$c_4$mim][$N(CN)_2$]; ■, [$c_4$mim][$C(CN)_3$]; ○, [$c_2$mim][SCN] [16]; △, [$c_2$mim][$N(CN)_2$] [16]; □, [$c_2$mim][$C(CN)_3$] [16]; (---), regression line.

group length increases, and free volume in ionic liquids increases and finally, these phenomena improve the solubility of CO_2 [15,30].

CONCLUSIONS

We measured bubble-point pressure of CO_2+ionic liquids ([$c_4$mim][$C(CN)_3$], [$c_4$mim][$N(CN)_2$] and [$c_4$mim][SCN]. The results of experiment show bubble-point pressure increases with increasing pressure and decreasing temperature. Furthermore, when we compared solubility of CO_2 containing different numbers of cyanide anion, [$C(CN)_3$]-anion in [c4mim]-cation based ionic liquids had the highest solubility of CO_2, while [SCN]-anion had the lowest one. This means that the cyanide anion enhances the CO_2 solubility in ionic liquid. Similarly, the longer alkyl chain group length is in cation, the higher solubility of CO_2 is obtained. In conclusion, combining the anion containing more numbers of cyanide with the cation having longer alkyl chain group will result in obtaining ILS with higher CO_2 solubility.

REFERENCES

1. R. D. Rogers and K. R. Seddon, *Science*, **302**, 792 (2003).
2. I. Krossing, J. M. Slattery, C. Daguenet, P. J. Dyson, A. Oleinikova and H. Weingärtner, *J. Am. Chem. Soc.*, **128**, 13427 (2006).
3. J. H. Davis Jr., *Chem. Lett.*, **33**, 1072 (2004).
4. L. A. Blanchard, D. Hancu, E. J. Beckman and J. F. Brennecke, *Nature*, **399**, 28 (1999).
5. M. J. Earle and K. R. Seddon, *Pure Appl. Chem.*, **72**, 1391 (2000).
6. M. Kohoutová, A. Sikora, Š. Hovorka, A. Randová, J. Schauer, M. Tišma, K. Setničková, R. Petričkovič, S. Guernik, N. Greenspoon and P. Izák, *European Polym. J.*, **45**, 813 (2009).
7. M. S. Benzagouta, I. M. AlNashef, W. Karnanda and K. Al-Khidir, *Korean J. Chem. Eng.*, **30**, 2108 (2013).
8. M. Armand, F. Endres, D. R. MacFarlane, H. Ohno and B. Scrosati, *Nature Mater.*, **8**, 621 (2009).
9. D. W. Kim, R. Roshan, J. Tharun, A. Cherian and D. W Park, *Korean J. Chem. Eng.*, **30**, 1973 (2013).
10. S. H. Ha and Y. M. Koo, *Korean J. Chem. Eng.*, **28**, 2095 (2011).
11. J. D. Figueroa, T. Fout, S. Plasynski, H. McIlvried and R. D. Srivastava, *Int. J. Greenh. Gas Control*, **2**, 9 (2008).
12. X. Zhang, X. Zhang, H. Dong, Z. Zhao, S. Zhang and Y. Huang, *Energy Environ. Sci.*, **5**, 6668 (2012).
13. K. E. Gutowski and E. J. Maginn, *J. Am. Chem. Soc.*, **130**, 14690 (2008).
14. J. F. Brennecke and E. J. Maginn, *AIChE J.*, **47**, 2384 (2001).
15. M. J. Muldoon, S. N. V. K. Aki, J. L. Anderson, J. K. Dixon and J. F. Brennecke, *J. Phys. Chem. B*, **111**, 9001 (2007).
16. J. E. Kim, H. J. Kim and J. S. Lim, *Fluid Phase Equilib.*, **367**, 151 (2014).
17. H. N. Song, B. C. Lee and J. S. Lim, *J. Chem. Eng. Data*, **55**, 891 (2010).
18. S. A. Kim, J. H. Yim and J. S. Lim, *Fluid Phase Equilib.*, **332**, 28 (2012).
19. J. H. Yim and J. S. Lim, *Fluid Phase Equilib.*, **352**, 67 (2013).
20. IEC BIPM, ISO IFCC and I IUPAC, *Guide to the Expression of Uncertainty in Measurement*, International Organization of Standardization (ISO), Geneva, Switzerland (1995).
21. J. M. Prausnitz, R. N. Lichtenthaler and E. G. de Azevedo, *Molecular Thermodynamics of Fluid-Phase Equilibria*, 3rd Ed., Prentice-Hall (1999).
22. M. O. McLinden, S. A. Klein, E. W. Lemmoon and A. P. Peskin, *Thermodynamic Properties of Refrigerants and Refrigerant Mixtures Database (REFPROP) V.6.01*, NIST, Gaithersburg (1998).
23. J. O. Valderrama and R. E. Rojas, *Ind. Eng. Chem. Res.*, **48**, 6890 (2009).
24. E. K. Shin and B. C. Lee, *J. Chem. Eng. Data*, **53**, 2728 (2008).
25. S. G. Nam and B. C. Lee, *Korean J. Chem. Eng.*, **30**, 474 (2013).
26. M. C. Kroon, E. K. Karakatsani, I. G. Economou, G. J. Witkamp and C. J. Peters, *J. Phys. Chem.*, **110**, 9262 (2006).
27. A.-L Revelli, F. Mutelet and J.-N. Jaubert, *J. Phys. Chem. B*, **114**, 12908 (2010).
28. P. J. Carvalho, V. H. Alvarez, I. M. Marrucho, M. Aznar and J. A. P. Coutinho, *J. Supercrit. Fluids*, **50**, 105 (2009).
29. D. R. MacFarlane, J. M. Pringle, K. M. Johansson, S. A. Forsyth and M. Forsyth, *Chem. Commun.*, **18**, 1905 (2006).
30. S. N. V. K. Aki, B. R. Mellein, E. M. Saurer and J. F. Brennecke, *J. Phys. Chem. B*, **108**, 20355 (2004).